

A Numerical Study of Evanescent Fields in Backward-Wave Slabs

M.K. Kärkkäinen,¹ S.A. Tretyakov,¹ S.I. Maslovski,¹ and P.A. Belov^{1,2}

¹*Radio Laboratory, Helsinki University of Technology, P.O. Box 3000, FIN-02015 HUT, Finland**

²*Physics Department, St. Petersburg Institute of Fine Mechanics and Optics, Sablinskaya 14, 197101, St. Petersburg, Russia*

(Dated: July 10, 2018)

Numerical study of evanescent fields in an isotropic backward-wave (BW) (double negative or “left-handed”) slab is performed with the FDTD method. This system is expected to be able to restore all spatial Fourier components of the spectrum of a planar source, including evanescent fields, realizing a “superlens”. The excitation of surface modes on the interfaces of the slab, which is the key process responsible for the sub-wavelength focusing, is numerically confirmed and the time-domain field behavior is studied. In particular, a numerical verification of the amplification of evanescent modes by an isotropic BW slab with $\epsilon_r = \mu_r = -1$ is provided.

PACS numbers: 02.70.Bf, 41.20.Jb, 77.22.Ch, 77.84.Lf

The resolution wave limit of any optical device is well known: it is impossible to resolve details smaller than half wavelength. The physical reason of this limitation comes from the fact that evanescent waves in the Fourier spectrum of an object exponentially decay in the direction from the object plane. The decay factor reads $\alpha = \sqrt{k_t^2 - k_0^2}$, where k_0 is the wavenumber in free space, and k_t is the wavenumber of Fourier components in the object plane. The faster the field varies in the object plane, the faster it decays in the direction normal to the object plane. However, it was recently found that a very special kind of lens made of a material with negative relative parameters $\epsilon_r = -1, \mu_r = -1$ (at a certain frequency) can “amplify” the evanescent part of the spectrum, thus opening a way to realize a “superlens” with sub-wavelength resolution [1, 2, 3].

The reason for this counterintuitive behavior is the fact that for a fixed frequency, an interface between free space and a backward-wave medium with $\epsilon_r = -1, \mu_r = -1$ supports surface waves with arbitrary propagation constants along the interface [4]. Indeed, the eigenvalue equation for surface modes (surface polaritons) on an interface between two isotropic media with parameters $\epsilon_{1,2}$ and $\mu_{1,2}$ reads

$$\frac{\sqrt{k_1^2 - k_t^2}}{\epsilon_1} + \frac{\sqrt{k_2^2 - k_t^2}}{\epsilon_2} = 0, \quad \text{TM modes} \quad (1)$$

$$\frac{\mu_1}{\sqrt{k_1^2 - k_t^2}} + \frac{\mu_2}{\sqrt{k_2^2 - k_t^2}} = 0, \quad \text{TE modes} \quad (2)$$

where indices 1,2 correspond to the two media. If $\epsilon_2 = -\epsilon_1$ and $\mu_2 = -\mu_1$, both 1 and 2 are identically satisfied for all propagation constants k_t along the interface. This means that any evanescent incident plane wave is exactly in phase with one of the eigenmodes of the surface wave spectrum. If the interface is infinite in space, the amplitude of the excited surface wave becomes infinite. The amplification of evanescent fields in backward-wave slabs utilizes this resonant excitation of waveguide modes with large propagation constants. The incident field excites an eigenmode of the slab that is

formed by two exponentially decaying field components inside the slab. The spectrum of eigenmodes traveling along a slab can be found from the expression for the reflection or transmission coefficients: they have singularities at the spectral points. For material parameters satisfying $\mu_r = -1$ and $\epsilon_r = -1$ the transmission coefficient equals simply $\exp(\alpha d)$, where α is the decay factor of an evanescent mode from the source and d is the slab thickness [1]. Thus, there is only one eigenmode, and that solution corresponds to infinitely large k_t and α . For larger values of α the excitation is closer to the resonance with this eigenmode, and the field amplitude excited in the slab waveguide is larger.

In paper [5], however, it has been concluded that if the width of the slab is limited, the restoration of fields is physically meaningless as it involves infinite energy. To clarify the behavior of the evanescent fields in a BW slab or a finite width, we study the fields from a source that creates *only* evanescent spectrum in the time domain with the finite-difference time-domain (FDTD) method. Time domain waveforms at suitably chosen observation points and snapshot field distributions are calculated. Our simulations show that the amplification indeed occurs, and it is due to the surface modes excited on the slab boundaries.

In any backward-wave medium the negative permittivity and permeability must be dispersive, and here we adopt the Lorentz model to account for the frequency dispersion. The expressions for the permittivity and permeability are of the form

$$\begin{aligned} \epsilon(\omega) &= \epsilon_0 \left(1 + \frac{\omega_{pe}^2}{\omega_{0e}^2 - \omega^2 + j\Gamma_e \omega} \right), \\ \mu(\omega) &= \mu_0 \left(1 + \frac{\omega_{pm}^2}{\omega_{0m}^2 - \omega^2 + j\Gamma_m \omega} \right). \end{aligned} \quad (3)$$

Here, ω_{0e} and ω_{0m} are the resonant frequencies of the material and Γ_e and Γ_m are the damping factors, which are assumed to be zero in numerical simulations. This model corresponds to a realization of BW materials as mixtures

of conductive spirals or omega particles, as discussed in [6]. In this artificial material both electric and magnetic polarizations are due to currents induced on particles of only one shape, which provides a possibility to realize the same dispersion rule for both material parameters, as in (3). Note that the medium realized by Smith *et. al.* is built using different principles [7]. Numerical techniques appropriate to simulations of a material with the above parameters with FDTD can be found in [8, 9, 10]. The discretization scheme used in this paper is described in detail in [10].

Let the interface between free space and a BW slab lie along the x -axis. The excitation plane (a line in our 2D cut) is located at a distance d_s from the BW slab of thickness d . In order to be able to study the behavior of the evanescent field, we excite a BW slab by a source which produces no traveling waves in the direction orthogonal to the source plane. We choose the incident electric field that depends on the x -coordinate along the interface and on the time t in the following manner:

$$E(x, t) = e^{-\left(\frac{x-x_0}{x_d}\right)^2} r(t) \cos(k_x x - \omega_0 t). \quad (4)$$

The ramp function $r(t)$ increases smoothly from 0 to 1 over about 50 periods of the cosine function. It is very important that the amplitude grows slowly enough; a rapid increase in the amplitude does not yield a constant amplitude on the second slab interface or in the image plane, because of a wide frequency spectrum of the source. x_0 is taken to be the x -coordinate in the middle of the slab and x_d determines the rate of decay of the incident electric field amplitude as measured from x_0 . ω_0 is the center angular frequency of the excitation. Due to

the finite simulation space, we have given a spatial profile to the incident field to obtain a decaying amplitude near the boundaries of the simulation space. The shape of the profile is the normal distribution. The incident fields propagate to $+x$ -direction along the interface but decay exponentially in the y -direction normal to the slab boundaries. From the dispersion relation in free space, $k_x^2 + k_y^2 = \omega^2/c^2$ we see that by choosing $k_x > \omega_0/c$ ($k_y = 0$) in (4) we obtain exponentially decaying fields away from the source in the y -direction. In our numerical simulations, we use $k_x = 13.62 \text{ m}^{-1}$ ($k_0 = 9.17 \text{ m}^{-1}$).

The problem space is two-dimensional, with the field components H_x, H_y , and E_z . The peak of the incident spectrum is at $\omega_0 = 2.75 \cdot 10^9 \text{ rad/s}$, and the parameters in (3) are the following: $\omega_{0e} = \omega_{0m} = 0.55 \cdot 10^9 \text{ rad/s}$, $\omega_{pe}^2 = \omega_{pm}^2 = 1.482 \cdot 10^{19} (\text{rad/s})^2$, $\Gamma_e = \Gamma_m = 0$. With these choices, we obtain $\epsilon(\omega) = \mu(\omega)$ for all ω and $\epsilon(\omega)/\epsilon_0 = \mu(\omega)/\mu_0 = -1$ at $\omega = \omega_0$. Absorbing boundary conditions (ABC) are used to terminate the computational domain at the outer boundaries of the lattice. For simplicity, we have used Liao's third order ABC [11], although more sophisticated ABC's are available. The use of usual ABC's requires a small gap between the outer boundary of the computational space and the BW material slab, since the Liao's ABC is not applicable to dispersive media. The reflection from the slab ends is negligible. We excite a slab of thickness $7\Delta y = 9 \text{ cm}$, carrying out the simulations in a 500×60 lattice. The source plane is located at a distance $d_s = 3.5\Delta y = 5.25 \text{ cm}$ from the boundary of the slab (tangential magnetic field components are defined on the interfaces). Determining the precise spatial profile of the source, we take $x_0 = 250\Delta x$ and $x_d = x_0/5$ in (4).

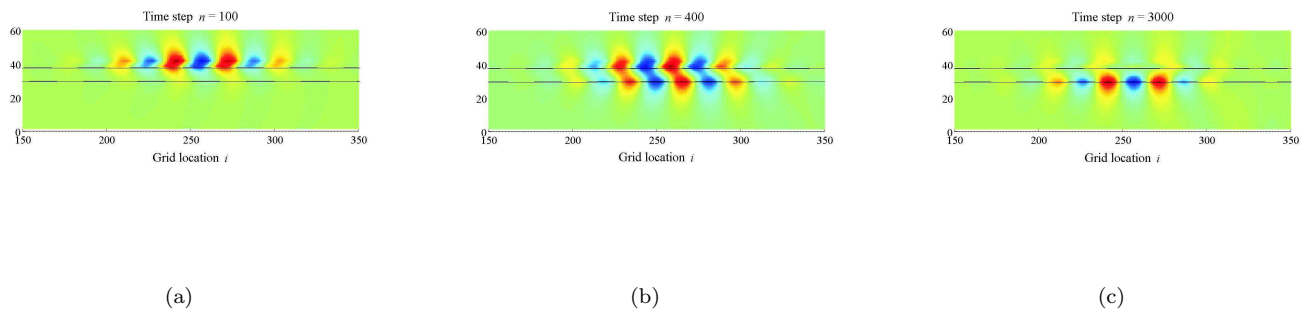


FIG. 1: (a) The source fields are visible above the slab. (b) The evanescent fields above the slab create surface waves on the boundaries of the slab. (c) The evanescent mode has been amplified by the slab: strong field amplitudes are visible on the second interface. The fields created by the source are barely visible above the slab, although they are just reaching the maximum amplitude.

The problem formulation described above enables us to study how the evanescent fields behave in a BW slab and how the surface modes are excited. The numerical results are presented and discussed next.

FDTD simulations have been run to see how the electric fields behave on the slab boundaries and inside the slab. The electric fields created by the source at an early stage of the simulation are seen in Figure 1 a). The snapshot electric field distribution in Figure 1 b) shows that the fields have passed through the slab and the field amplitudes on the slab boundaries are high. The electric field distribution in Figure 1 c) is recorded at a later moment of time. Figure 1 c) reveals that the electric fields are much stronger on the second interface than on the first interface. Evidently, the excited evanescent mode is amplified by the slab. Notice that the source is just reaching its maximum amplitude at $n = 3000$, although the fields created by the source are not visible in Figure 1 c) due to the scaling.

Next we record the electric fields as a function of time at some observation points. All the observation points are on the line $x = 250\Delta x$: one in the middle of the slab, another on the lower interface and the third in air in the image plane, which is located at the distance $d - d_s$ from the second interface. The electric fields at these points as functions of time are shown in Figures 2 and 3. Figure 2 shows that the electric field amplitude is larger on the lower boundary of the slab than inside the slab. The incident electric field amplitude in the source plane is equal to unity. The source and the observation point inside the slab are located at equal distances from the upper slab boundary. Therefore, it is expected that the electric field amplitude in the middle of the slab is equal to 1. We have observed a smaller amplitude in the middle of the slab. The incident electric fields and the fields in the image plane are compared in Figure 3. From the theory, it is expected that the electric field amplitude in the image plane equals the incident electric field amplitude. The fields in the source plane and in the image plane are quite close to each other, see Figure 3.

Let us now compare the results in Figure 2 with analytical results. The evanescent mode decays away from the source plane as a function of distance y by a factor of

$$T_1 = e^{-\sqrt{k_x^2 - k_0^2}y} \quad (5)$$

until it hits the upper boundary of the slab. In the slab of thickness d , the fields are amplified by a factor of

$$T_2 = e^{\sqrt{k_x^2 - k_0^2}d}. \quad (6)$$

Combining these factors, we obtain the transmission coefficient from the source plane to the second interface as

$$T = e^{\sqrt{k_x^2 - k_0^2}(d - d_s)}, \quad (7)$$

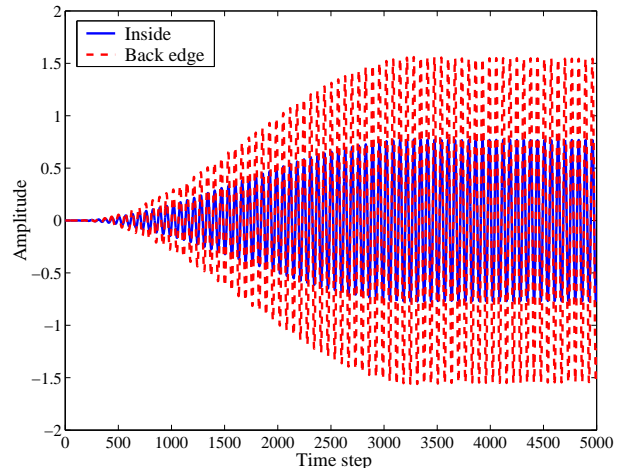


FIG. 2: The electric field amplitude on the second boundary of the slab is larger than that of the source field, and also larger than the amplitude in the middle of the slab. This result verifies that the evanescent fields are amplified by the slab.

where d_s is the distance of the source from the upper boundary of the slab. Substituting the parameters we obtain $T \approx 1.69$. In the numerical simulations, the maximum ratio of the field amplitudes on the lower interface and on the source plane equals 1.56, being of the same order as the analytical result. The fact that the calculated value is smaller should have been expected, because in the numerical model the incident field amplitude decays from the slab center, while the estimation is for the plane-wave excitation.

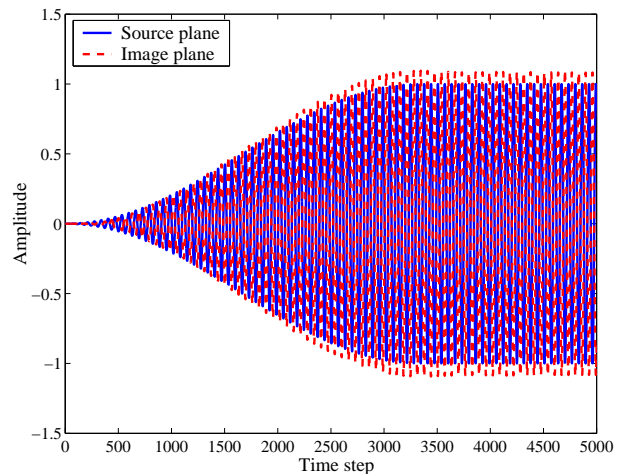


FIG. 3: The evanescent electric fields in the image plane are close to the fields in the source plane. This is also in agreement with the theory.

We have numerically demonstrated that the evanescent modes are amplified in a lossless frequency dispersive backward-wave slab. The field amplitude at the other

side of the slab is larger than the source amplitude, and the “amplification ratio” agrees well with the analytical estimation. The numerically observed electric fields in the image plane approximately reconstruct the source fields above the slab. Thus, our numerical results support the conclusion of paper [1] based on the theoretical analysis of an infinite lossless backward-wave slab. The conclusion of [5] about infinite field energy required for the restoration of evanescent fields in finite slabs has no theoretical ground (since the slab dimensions are finite and the field amplitudes are finite everywhere if all the wavenumbers in the spectrum are finite) and is in conflict with the results of numerical simulations.



* Electronic address: mkk@cc.hut.fi

[1] J. Pendry, Phys. Rev. Lett. **85**, 3966 (2000).

[2] J. Pendry and S. Ramakrishna, J. Phys. Condens. Matter **14**, 8463 (2002).

[3] S. Ramakrishna, J. Pendry, M. Wiltshire, and W. Stewart, cond-mat/0207026 (2002).

[4] S. Tretyakov, S. Maslovski, I. Nefedov, and M. Kärkkäinen, cond-mat/0212393 (2003).

[5] N. Garcia and M. Nieto-Vesperinas, Phys. Rev. Lett. p. 207403 (2002).

[6] S. Tretyakov, I. Nefedov, C. Simovski, and S. Maslovski, *Advances in Electromagnetics of Complex Media and Metamaterials* (Kluwer Academic Publishers, 2003), p. 99.

[7] D. Smith, W. Padilla, D. Vier, S. Nemat-Nasser, and S. Schultz, Phys. Rev. Lett. **84**, 4184 (2000).

[8] A. Taflov and S. Hagness, *Computational Electrodynamics – The finite-difference time-domain method* (Artech House, Boston, 2000).

[9] J. Young and R. Nelson, IEEE Antennas Propag. Magazine **43**, 72 (2001).

[10] M. Kärkkäinen and S. Maslovski, Microw. and Opt. Tech. Lett. **5**, 129 (2003).

[11] Z. Liao, H. Wong, B.-P. Yang, and Y.-F. Yuan, Sci. Sin. Ser. A p. 1063 (1984).